A&A 436, 1–8 (2005)
DOI: 10.1051/0004-6361:20047115

Astronomy & Astrophysics

The orbital resonance model for twin peak kHz quasi periodic oscillations in microquasars⋆

G. Török[1,2], M. A. Abramowicz[1,2,3], W. Kluźniak[1,4,5], and Z. Stuchlík[2]

[1] UKAFF supercomputer facility, Department of Physics and Astronomy, University of Leicester, UK
[2] Institute of Physics, Faculty of Philosophy and Science, Silesian University in Opava, Bezručovo nám. 13, 746 01 Opava, Czech Republic
e-mail: terek@volny.cz, stu10uf@fpf.slu.cz
[3] Astrophysics, Göteborg University, 412-96 Göteborg, Sweden
e-mail: marek@fy.chalmers.se
[4] Institute of Astronomy, Zielona Góra University ul. Lubuska 2, 65-265 Zielona Góra, Poland
[5] Copernicus Astronomical Centre, Warszawa, Poland
e-mail: wlodek@camk.edu.pl

Received 21 January 2004 / Accepted 13 January 2005

Abstract. In all microquasars with double peak high frequency QPOs, the ratio of the frequencies is 3:2, which supports the suggestion that a non-linear resonance between two modes of oscillation in the accretion disk plays a role in exciting the observed modulations of the X-ray flux. We discuss evidence in favor of this interpretation and relate the black hole spin to the frequencies expected for various types of resonances that may occur in nearly Keplerian disks in strong gravity. For those microquasars where the mass of the central X-ray source is known, the black hole spin can be deduced from a comparison of the observed and expected frequencies.

Key words. black hole physics – X-rays: binaries

1. Introduction

Many Galactic black hole and neutron star sources in low-mass X-ray binaries show QPOs (quasi periodic oscillations) in their observed X-ray fluxes, i.e., peaks in the Fourier variability power density spectra. QPOs have attracted a lot of attention, mostly because of their high frequencies. In fact, the frequencies of some QPOs are in the kHz range which corresponds to orbital frequencies just a few gravitational radii away from the central black hole or neutron star. Thus, super-strong Einstein's gravity is most likely to be directly involved here.

Observed properties of QPOs have a very rich and complex phenomenology, as reviewed by van der Klis (2000) and McClintock & Remillard (2003). A special class of high frequency QPOs consists of double peak QPOs, i.e., those which show a pair of peaks in their power density spectra, corresponding to two frequencies $\nu_{\rm upp}$, $\nu_{\rm down}$. It was realized (Abramowicz & Kluźniak 2001; Kluźniak & Abramowicz 2002; McClintock & Remillard 2003; see also Table 1 and its references) that typically the two frequencies, $\nu_{\rm upp}$, $\nu_{\rm down}$, form rational ratios and that most often $\nu_{\rm upp}/\nu_{\rm down} = 3/2$. In all four microquasars in which double peak QPOs have been discovered so far, the frequency ratio is amazingly close to $3/2$ (see Table 1 and Fig. 1).

It is quite natural to ask whether one could find a physical reason for the $3/2$ ratio. Kluźniak, Abramowicz and collaborators argue that the $3/2$ ratio, along with other general properties of the double peak QPOs, reflect a non-linear resonance between epicyclic oscillations in accretion fluid flows in super-strong gravity (first suggested by Kluźniak & Abramowicz 2000, 2001)[1]. Here we give a short summary of what has been done so far and present the results that can be directly related to observational data. For a recent review see Kluźniak & Abramowicz (2004) or, in more detail Abramowicz et al. (2004b).

The orbital resonance model demonstrates (Kluźniak & Abramowicz 2002) that *fluid accretion flows* (both Newtonian and relativistic) admit two linear quasi-incompressible modes of oscillations, vertical and radial, with coresponding eigenfrequencies equal to vertical and radial epicyclic frequencies for free particles[2]. Although this is a very generic property of

⋆ Appendix A is only available in electronic form at http://www.edpsciences.org

[1] For a possible mechanism of X-ray modulation see Bursa et al. (2004); Bursa (2004).

[2] This point is sometimes misunderstood. Some critics of the orbital resonance model appear to wrongly believe that the model is based

Table 1. Frequencies of twin peak kHz QPOs in microquasars (after McClintock & Remillard 2003).

Source	$\nu_{\rm upp}$ [Hz]	$\Delta\nu_{\rm upp}$ [Hz]	$\nu_{\rm down}$ [Hz]	$\Delta\nu_{\rm down}$ [Hz]	$2\nu_{\rm upp}/3\nu_{\rm down}-1$	Mass$^{(e)}$ [$M_\odot$]
[a]GRO 1655–40	450	±3	300	±5	0.00000	6.0–6.6
[b]XTE 1550–564	276	±3	184	±5	0.00000	8.4–10.8
[c] H 1743–322	240	±3	166	±8	–0.03614	not measured
[d]GRS 1915+105	168	±3	113	±5	0.00885	10.0–18.0

[a] Twin peak kHz QPOs reported by Strohmayer (2001).
[b] Twin peak kHz QPOs reported by Remillard et al. (2002).
[c] Twin peak kHz QPOs reported by Homan et al. (2003). McClintock & Remillard (2004), state $\nu_{\rm upp}/\nu_{\rm low} = 242\,(\pm3\,{\rm Hz})\,/166\,(\pm5\,{\rm Hz})$.
[d] Twin peak kHz QPOs reported by Remillard et al. (2003).
[e] See Greene et al. (2001); Orosz et al. (2002); Greiner et al. (2001), and McClintock & Remillard (2003).

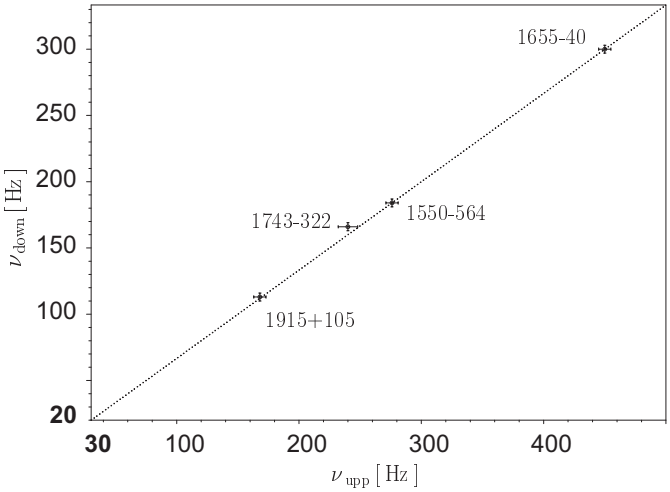

Fig. 1. In all four microquasars with twin peak kHz QPOs discovered, $\nu_{\rm upp}/\nu_{\rm down} = 3/2$.

general accretion flows, the idea may be best illustrated in the particular case of a fluid slender torus, i.e., a torus with the cross-section radius much smaller than the major radius. Such tori are commonly used to model accretion flows, e.g., a sequence of slender tori is involved in the warped disk models developed by Pringle (1997) and collaborators. Kluźniak & Abramowicz (2002) demonstrated that the vertical mode corresponds to a periodic displacement in which the whole torus moves as a rigid body up and down the equatorial plane, i.e., each fluid element has a vertical velocity that periodically changes in time, but does not depend on the position. The frequency of the mode is equal to the vertical epicyclic frequency that a fictitious free particle would have if orbiting the circle of maximum pressure in the torus equilibrium position. There is a similar epicyclic radial mode with the eigenfrequency equal to the radial epicyclic frequency of the ficticious free particle at the central pressure circle, in which the oscillating fluid elements oscillate with velocities that are parallel to the plane, depend on time but not on position. In the linear regime these two modes are formally uncoupled. However, in a more realistic description, one should take into account non-linear effects that certainly occur in fluids due to pressure, dissipation, etc. It was shown that non-linear effects couple the two epicyclic (and other) modes. When conditions are right, this may result in a resonance (Kluźniak & Abramowicz 2002).

This general ideas briefly described above were followed up by extensive and detailed analytic analysis (Rebusco 2004a,b; Horák 2004; Horák et al. 2004), as well as by numerical simulations (Abramowicz et al. 2003), which show that a few generic types of non-linear orbital resonances consistent with the 3/2 ratio are possible. Among them, the parametric resonance between vertical and radial epicyclic modes in strong gravity is perhaps the most interesting, because it *necessarily* gives the 3/2 ratio. Other resonances give the 3/2 ratio, but other ratios $m/n\,(n,\ m = 1, 2, 3, \ldots)$ as well.

At the present stage of development of the model, specific physical mechanisms that may excite a particular resonance have not yet been clearly identified. Mathematically, it was proved that in a particular range of an adjustable parameter, the resonance model explains the case in which the frequency ratio is fairly fixed at the 3/2 value, as for microquasar QPOs (Horák 2004). For a different range of the parameter, the model reproduces varying frequencies $\nu_{\rm upp}$ and $\nu_{\rm down}$, accurately following the whole path observed in the case of ScoX-1 QPOs (Abramowicz et al. 2003; Rebusco 2004a).

Despite these and several other uncertainties, the resonance model may be accurately checked and tested, because it makes clear and precise predictions about the values of frequencies of oscillations when they do not vary. This case is reminiscent of high frequency double peak QPOs observed in microquasars.

In this paper, we discuss frequency predictions of the orbital resonance model for microquasars. For predicted eigenfrequencies of different types of resonances, we calculate black hole masses in the full range of possible black hole spins (i.e., corresponding to the Kerr parameter varying between $a = -1$ to $a = +1$). We then compare results of these theoretical predictions with the observed QPOs frequencies and with observationally estimated black hole masses.

on *free particle* motion. We stress that the model describes *fluid oscillations* of accretion flows with eigenfrequencies equal to epicyclic frequencies of free particles. These free particles are not present in the flow, but are only introduced for mathematical convenience.

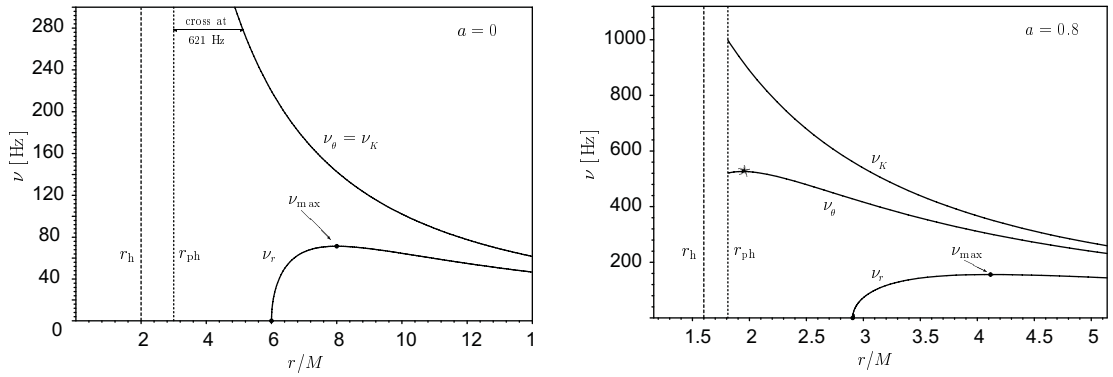

Fig. 2. Orbital frequency $\nu_{\rm K}$ and the two epicyclic frequencies, radial ν_r, and vertical ν_θ, for Keplerian circular orbits around a 10 $M_\odot$ black hole. Such orbits are possible only for radii larger than the radius of the circular photon orbit $r_{\rm ph}$. This limit is labelled here and in other figures by the subscript ph. Left panel for non-rotating black hole, right panel for a moderately ($a = 0.8$) rotating one. In Newton's theory with the $1/r$ potential, all three frequencies are equal: $\nu_{\rm K} = \nu_\theta = \nu_r$. Strong Einstein's gravity makes $\nu_\theta > \nu_r$, and $\nu_{\rm K} \geq \nu_\theta$ for $a \geq 0$.

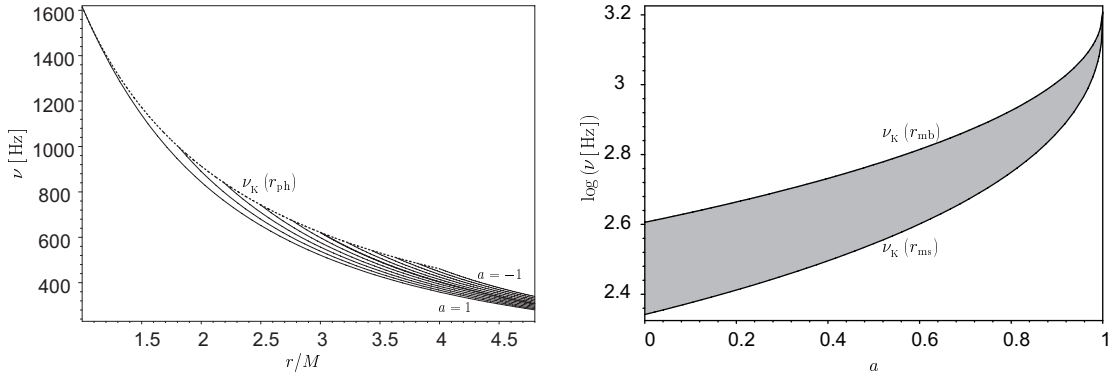

Fig. 3. *Left*: the Keplerian orbital frequency for a 10 $M_\odot$ mass black hole. The curves are spaced every 0.2 in a. *Right*: RISCO and ISCO frequencies for a 10 $M_\odot$ mass black hole. The accretion disk inner edge must be located between RISCO and ISCO, depending on the disk's efficiency.

2. Orbital frequencies

Three orbital frequencies are relevant to our discussion of the resonance model in this paper: Keplerian orbital frequency $\nu_{\rm K} = \Omega_{\rm K}/2\pi$, vertical epicyclic frequency $\nu_\theta = \omega_\theta/2\pi$, and radial epicyclic frequency $\nu_r = \omega_r/2\pi$.

For the Kerr black hole[3], they are given in terms of the corresponding angular velocities $\Omega_{\rm K}$, ω_θ, ω_r by well-known formulae (e.g., Nowak & Lehr 1999)

$$\begin{aligned}
\Omega_{\rm K} &= \left(\frac{GM_0}{r_G^3}\right)^{1/2} \left(x^{3/2} + a\right)^{-1}, \\
\omega_\theta^2 &= \Omega_{\rm K}^2 \left(1 - 4\,a\,x^{-3/2} + 3a^2\,x^{-2}\right), \\
\omega_r^2 &= \Omega_{\rm K}^2 \left(1 - 6\,x^{-1} + 8\,a\,x^{-3/2} - 3\,a^2\,x^{-2}\right),
\end{aligned} \tag{1}$$

where $x = r/M$. The two epicyclic frequencies, vertical $\nu_\theta = \omega_\theta/2\pi$ and radial $\nu_r = \omega_r/2\pi$, are shown in Fig. 2 together with the Keplerian orbital frequency $\nu_{\rm K} = \Omega_{\rm K}/2\pi$ for a nonrotating ($a = 0$) black hole and for a moderately rotating ($a = 0.8$) black hole. Figures 3 and 4 show these frequencies in the whole range of a from a maximally co-rotating black hole ($a = 1$) to a maximally counter-rotating black hole ($a = -1$).

[3] We rescale the black hole mass with $M = GM_0/c^2 = r_{\rm G}$, and the black hole angular momentum with $a = J_0 c/{\rm G}M_0^2$ and use Boyer-Lindquist coordinates, t, r, θ, ϕ.

2.1. The highest possible orbital frequency: ISCO and RISCO

In Newton's theory with $-GM_0/r$ potential, $GM_0/r^{3/2} = \nu_{\rm K} = \nu_r = \nu_\theta$; but in the strong gravity of a rotating black hole, $\nu_\theta > \nu_r$. Also, $\nu_{\rm K} > \nu_\theta$ for co-rotating orbits, i.e., ones rotating in the same sense as the black hole. The radial epicyclic frequency ν_r has a maximum at a particular circular orbit with radius $r > r_{\rm ms}$, depending on the black hole spin (Okazaki et al. 1987), and goes to zero at $r_{\rm ms}$, the marginally stable circular orbit. The orbit is now most often called ISCO, which is a handy short name, and we suggest to call RISCO the marginally bound orbit at $r_{\rm mb}$.

The location of the inner edge of accretion disk, and therefore also the value of the highest possible orbital frequency, depends on the disk's radiative efficiency. Very thin disks with high radiative efficiency have their inner edges almost exactly at ISCO. Correspondingly, the ISCO orbital frequency, $\nu_{\rm K}(r_{\rm ms})$, is the highest possible orbital frequency for thin disks, and also the highest possible QPO frequency caused by inhomogeneities orbiting within a thin disk (Kluźniak et al. 1990). On

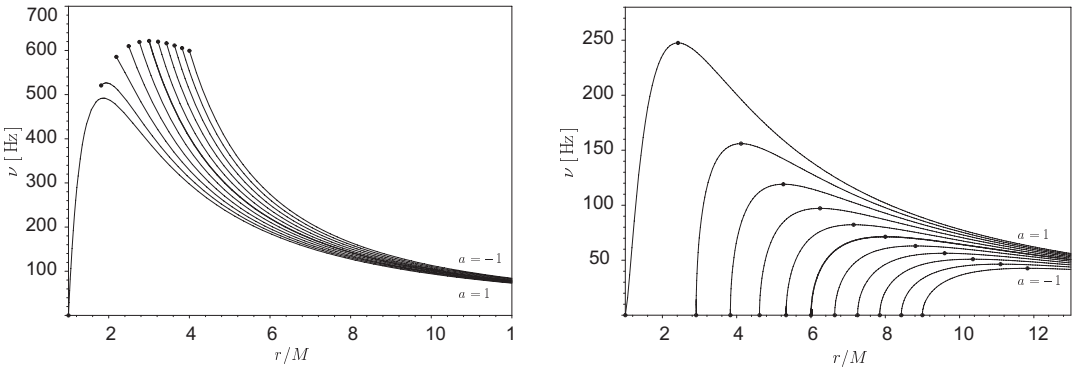

Fig. 4. *Left*: the vertical epicyclic frequency for a 10 $M_\odot$ mass black hole. The curves terminate at the photon orbit. *Right*: the radial epicyclic frequency for 10 $M_\odot$ mass black hole. Maximal values are also indicated. In both panels, consecutive curves differ in a by 0.2.

the other hand, for accretion disks with low radiative efficiency such as radiative and ion tori, slim disks, and adafs, the orbits are stabilized by the pressure gradient, and the inner edge approaches RISCO as was first proved analytically by Kozłowski et al. (1978) and then confirmed in numerical simulations by many authors. For such disks, the highest possible orbital frequency is obviously higher than the orbital frequency at ISCO, $\nu_{\rm K}(r_{\rm mb}) > \nu_{\rm K}(r_{\rm ms})$, as illustrated in Fig. 3 (right panel).

3. Possible orbital resonances

In thin black hole accretion disks, matter spirals down the central black hole along streamlines that are located almost on the black hole equatorial plane $\theta = \theta_0 = \pi/2$ and that locally differ only slightly from a family of concentric circles $r = r_0 = \text{const}$. For a fictitious, strictly Keplerian flow that is nonetheless mathematically convenient (i.e., circular free particle motion) the small deviations ($\delta r = r - r_0$, $\delta\theta = \theta - \theta_0$) are governed in the linear regime by the equations

$$\delta\ddot{r} + \omega_r^2\,\delta r = 0, \quad \delta\ddot{\theta} + \omega_\theta^2\,\delta\theta = 0, \tag{2}$$

where dot stands for time derivative. Obviously, this represents epicyclic oscillations with eigenfrequencies ω_θ, ω_r given by Eqs. (1). The analysis is not restricted to thin disks. These equations also describe the position of a fiducial circle of a slim torus undergoing small oscillations.

In a more realistic physical model, one considers equations for small deviations of fluid streamlines from planar circular motion governed by a set of equations (Abramowicz et al. 2003; Horák 2004),

$$\begin{aligned}\delta\ddot{r} + \omega_r^2\,\delta r &= \omega_r^2 f_r(\delta r, \delta\theta, \delta\dot{r}, \delta\dot{\theta}),\\ \delta\ddot{\theta} + \omega_\theta^2\,\delta\theta &= \omega_\theta^2 f_\theta(\delta r, \delta\theta, \delta\dot{r}, \delta\dot{\theta}).\end{aligned} \tag{3}$$

Here f_r and f_θ are some general non-linear functions of their arguments. Assuming a specific and detailed physical model of accretion flow, one could write down the specific forms of f_r and f_θ and solve Eqs. (3) to get the oscillatory behavior of the flow that, hopefully, may explain the observed QPOs. This is, however, not necessarily the best strategy. There is no consensus on details of the physics of accretion, especially on those details that are connected to dissipation, and details are of course very relevant here. Thus, if the assumed particular model is not sufficiently realistic in relevant details, the corresponding f_r and f_θ will not be sufficiently realistic either.

A safer strategy, but technically more difficult because of its mathematical complexity, would be to keep f_r and f_θ general and study general mathematical properties of the equations. In this way, one should be able find several (if not all) possible behaviours that are similar to those of observed QPOs before trying to find a physical interpretation of the mathematical model a posteriori. This strategy was adopted by Abramowicz et al. (2003) and Horák et al. (2004). Here we briefly describe only some essential points.

3.1. The 3:2 parametric resonance

The simplest possibility is that the two observed QPO frequencies correspond directly to the epicyclic frequencies in a 3:2 ratio. This condition holds at a particular radius $r_{3:2}(a)$, determined by the condition $3\omega_r(r_{3:2}, a) = 2\omega_\theta(r_{3:2}, a)$ and Eq. (1).We show function $r_{3:2}(a)$ in Fig. 5. The 3:2 ratio of frequencies has a natural explanation in relativistic hydrodynamics for a nearly Keplerian fluid motion expanded to the lowest order: the radial epicyclic mode can excite the vertical epicyclic mode in a parametric resonance (Kluźniak & Abramowicz 2002). One could argue that vertical motion is described by the Mathieu equation which is well-known to describe a parametric resonance (Landau & Lifshitz 1976)

$$\delta\ddot{\theta} + \omega_\theta^2\,[1 + h\cos(\omega_r t)]\,\delta\theta = 0. \tag{4}$$

This can be formally derived from Eqs. (3) with a particular choice of f_r and f_θ, corresponding to (see, e.g., Rebusco 2004a)

$$\delta\ddot{r} + \omega_r^2\,\delta r = 0, \quad \delta\ddot{\theta} + \omega_\theta^2\,\delta\theta = -\omega_\theta^2\,\delta\theta\,\delta r. \tag{5}$$

The first equation describes radial epicyclic oscillations and has a solution $\delta r = h\cos(\omega_r t)$. Substituting it in the second equation, one gets Eq. (4).

From the theory behind the Mathieu equation one knows that the parametric resonance is excited when

$$\frac{\omega_r}{\omega_\theta} = \frac{\nu_r}{\nu_\theta} = \frac{2}{n}, \quad n = 1, 2, 3\ldots \tag{6}$$

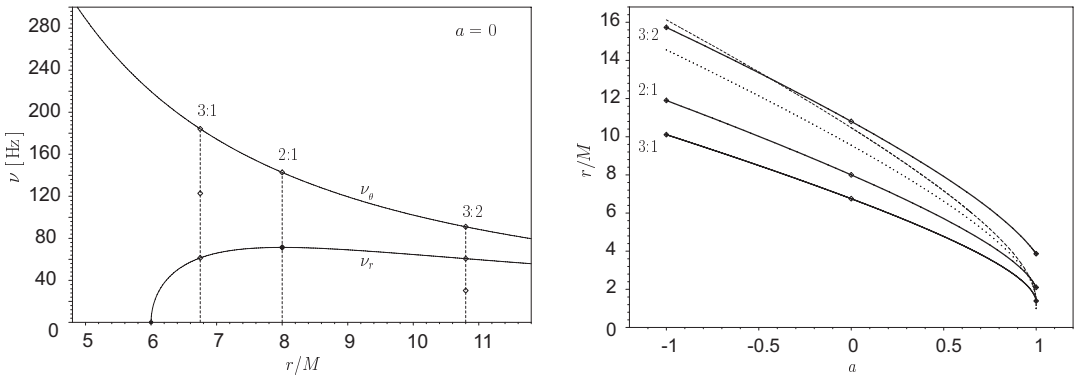

Fig. 5. *Left*: locations of three resonances between epicyclic motions in Schwarzschild metric: the 3:2 parametric, and the 2:1 and 3:1 forced cases. *Right*: these locations depend on the black hole spin. Also shown is the radius r_F (dotted line), at which the standard relativistic Shakura-Sunyaev disk (Page & Thorne 1974) locally emits the maximal flux, and the radius r_C (dashed line) corresponding to the pressure centre of the maximally thick torus, i.e., the torus with constant angular momentum density equal to the Keplerian value at RISCO.

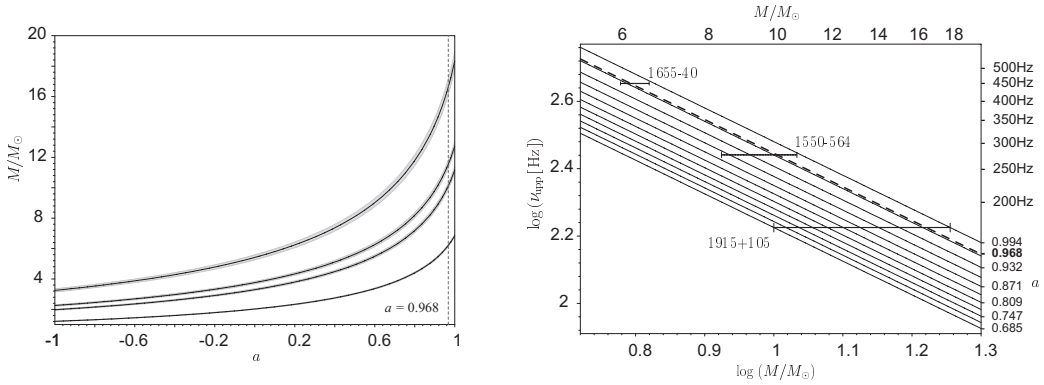

Fig. 6. Mass-spin dependence $M(a)$ (*left panel*) calculated (and shown in a range from two to twenty solar mass) from the 3:2 parametric resonance model for the frequencies ν_{upp} = 168 Hz, 242 Hz, 276 Hz, and 450 Hz (curves from the top in this order) observed in four microquasars (Table 1). Shadows show the range ±5 Hz The vertical dashed line denotes spin associated with the observational fit (7) – see right panel which shows in detail how the predicted spin for this 3:2 parametric resonance (i.e., curves in the left panel) fits the observational data (for error bars, see Table 1 and its references). The dashed line corresponds to the observational fit (7), implying spin $a \doteq 0.97$. One should notice that the deduced black hole spins are really rather high, which is expected if microquasar jets are a signature of large spin of the central black hole.

and is strongest for the smallest possible value of n (Landau & Lifshitz 1976). Because near black holes $\nu_r < \nu_\theta$, the smallest possible value for resonance is $n = 3$, which means that $2\,\nu_\theta = 3\,\nu_r$. This explains the observed 3:2 ratio, assuming $\nu_{upp} = \nu_\theta$ and $\nu_{down} = \nu_r$.

It turns out that the same condition (6) holds also for internal resonance in a system with conserved energy. A resonance of the type discussed above was found in numerical simulations of oscillations in a nearly Keplerian accretion disk by Abramowicz et al. (2003). Their numerical results were reproduced in exact analytic solutions first by Rebusco (2004a) and later confirmed and generalised by Horák (2004). The analytic solution is accurate up to fourth order terms in δr, $\delta\theta$, and based on the method of multiple scales (see, e.g., Nayfeh & Mook 1979). Existence of the 3:2 internal resonance is therefore a mathematical property of thin, nearly Keplerian disks. Of course in real disks neither $\delta r = A_0 \cos(\omega_r t)$ nor $\delta a_\theta = 0$ exactly; but one may expect that because these equations are approximately obeyed for thin disks, parametric resonance will also be excited in realistic situations. This is indeed the case. It was found that the resonance is excited in the non-Keplerian case with some weak forces $\delta a_\theta \neq 0$ and $\delta a_r \neq 0$ present. Their origin is certainly connected to stresses (pressure, magnetic field, viscosity), but exact details remain to be determined – at present δa_θ and δa_r are not calculated from first principles but described by an ansatz[4].

In Fig. 6 (left panel) we illustrate for the 3:2 resonance the theoretically predicted mass-spin combinations for four representative (observed) frequencies ν_{upp} (Table 1); on the right panel are these predictions compared with observational limitations of mass and the fit found by McClintock & Remillard (2003):

$$\nu_{upp} = 2.793 \left(\frac{M_0}{M_\odot}\right)^{-1} \text{ kHz}. \qquad (7)$$

[4] While the lack of a full physical understanding is obviously not satisfactory, experience tells that such a situation is not uncommon for non-linear systems. Examples are known of mathematically possible resonances causing damage in bridges, airplane wings, etc., for which no specific physical coupling mechanism could be pinned down (Nayfeh & Mook 1979).

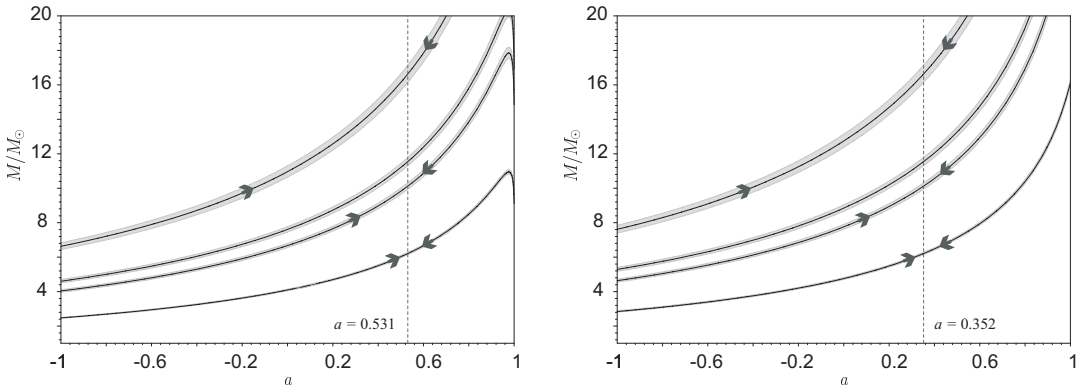

Fig. 7. Mass-spin dependence $M(a)$ calculated (and shown in range from two to twenty solar mass) from 3:1 (*left panel*) and 2:1 (*right panel*) forced resonance models for the frequencies $\nu_{\rm upp}$ = 168 Hz, 242 Hz, 276 Hz, and 450 Hz (curves from the top in this order) observed in four microquasars (Table 1). Shadows show the range ±5 Hz. Vertical dashed lines denote spin associated with the observational fit (7), arrows indicate the observationally given range of mass for the source (in the case of H 1743-322 [i.e. 242 Hz] the mass is not established yet). Both resonances are between vertical and radial epicyclic oscillations.

3.2. Forced 3:1 and 2:1 resonances

A direct resonant forcing of vertical oscillations by the radial ones through a pressure coupling, and with $\delta a_r \sim \cos(\omega_r t)$, was evident in recent numerical simulations of oscillations of a perfect fluid torus (Lee et al. 2004). This supports the idea (Abramowicz & Kluźniak 2001) for another possible model for the twin peak kHz QPOs: a forced non-linear oscillator,

$$\delta\ddot{\theta} + \omega_\theta^2 \delta\theta + [\text{non linear terms in } \delta\theta] = h(r)\cos(\omega_r t),$$
$$\omega_\theta = \left(\frac{p}{q}\right)\omega_r, \tag{8}$$

where p, q are small natural numbers. Obviously, the case of p:q = 3:2 corresponds to the same frequencies and radius as in the case of 3:2 parametric resonance ($\nu_{\rm upp} = \nu_\theta$, $\nu_{\rm down} = \nu_r$). The non-linear terms allow the presence of combination frequencies in resonant solutions for $\delta\theta(t)$ (see, e.g., Landau & Lifshitz 1976), which in the simplest case are

$$\omega_- = \omega_\theta - \omega_r, \quad \omega_+ = \omega_\theta + \omega_r. \tag{9}$$

As noticed by Abramowicz & Kluźniak (2001), these combination frequencies may be in the 3:2 ratio for p:q = 2:1, or p:q = 3:1 forced resonances. Simple arithmetic shows that in these two cases the observed frequencies $\nu_{\rm down} = \omega_{\rm down}/(2\pi)$ and $\nu_{\rm upp} = \omega_{\rm upp}/(2\pi)$ are uniquely given by,

$$\omega_{\rm down} = \omega_- = 2\,\omega_r, \quad \omega_{\rm upp} = \omega_\theta = 3\,\omega_r$$
$$\text{for } \frac{p}{q} = 3 \text{ forced epicyclic resonance}, \quad \omega_\theta = 3\,\omega_r, \tag{10}$$
$$\omega_{\rm upp} = \omega_+ = 3\,\omega_r, \quad \omega_{\rm down} = \omega_\theta = 2\omega_r$$
$$\text{for } \frac{p}{q} = 2 \text{ forced epicyclic resonance}, \quad \omega_\theta = 2\,\omega_r. \tag{11}$$

We illustrate mass-spin combinations implied by the forced epicyclic 3:1 and 2:1 resonance in Fig. 7.

3.2.1. Other possible combinations of frequencies giving the 3:2 ratio by forced resonance

In the previous subsection, the *full set* of possible forced resonances between epicyclical frequencies ν_θ and ν_r giving the observed 3:2 ratio was presented for $p, q < 4$. Of course, one can consider other combinations of ω_r, ω_θ, ω_- and ω_+ giving the same observed ratio[5]. But obviously the amplitude of oscillations is decreasing with increasing p, q (Landau & Lifshitz 1976). Nevertheless, let us note that, for higher integral numbers, forced resonances may be located much closer to the inner edge of the accretion disk than in the case of the parametric resonance, i.e.,

$$\omega_{\rm down} = \omega_- = 4\,\omega_r, \quad \omega_{\rm upp} = \omega_+(6/5)\,\omega_\theta = 6\,\omega_r$$
$$\text{for } p/q = 5/1 \quad \text{forced epicyclic resonance} \quad \omega_\theta = 5\,\omega_r. \tag{12}$$

For comparison also two examples of forced resonance are discussed with values of (p/q) being rational (and not integral) number:

$$\omega_{\rm down} = \omega_r, \quad \omega_{\rm upp} = \omega_- = (3/5)\,\omega_\theta$$
$$\text{for } p/q = 5/2 \text{ forced epicyclic resonance } \omega_\theta = (5/2)\,\omega_r, \tag{13}$$

$$\omega_{\rm down} = \omega_- = (2/3)\,\omega_r, \quad \omega_{\rm upp} = \omega_r = (3/5)\,\omega_\theta$$
$$\text{for } p/q = 5/3 \text{ forced epicyclic resonance } \omega_\theta = (5/3)\,\omega_r. \tag{14}$$

Corresponding resulting values of the black hole mass as a function of the rotational parameter a are given in the Appendix (Tables A.7–A.9).

3.3. "Keplerian" resonances

The resonances discussed so far were due to coupling between epicyclic oscillations – radial and vertical. Such coupling exists in a variety of realistic physical situations. It is more difficult to imagine a realistic physical coupling between radial epicyclic oscillations and orbital Keplerian oscillations. One possibility is connected to the fact that for a particular case of g-modes (Kato 2001a), the co-rotation resonance may occur. However, the co-rotation resonance leads to damping, not excitation, of modes (see Kato 2001b). In addition, observed

[5] Generally $\omega_{\rm upp}, \omega_{\rm down}$ are allowed in the form $m\,\omega_\theta + n\,\omega_r$, where m, n are integral numbers.

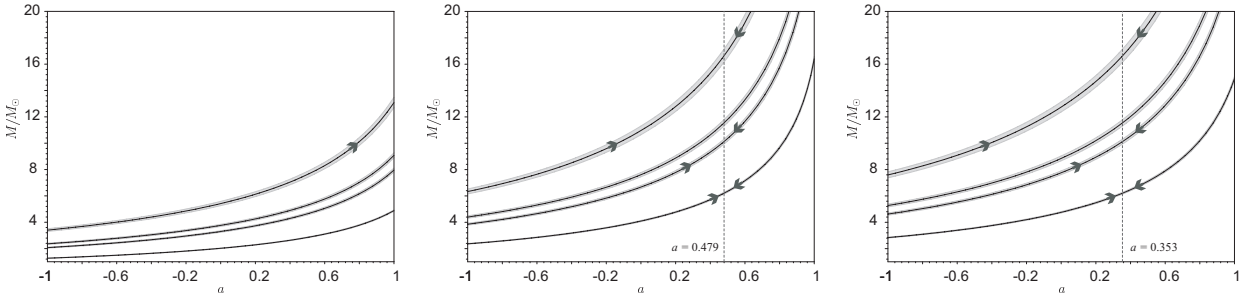

Fig. 8. Mass-spin dependence $M(a)$ calculated in the "Keplerian" resonance model in the range of two to twenty solar masses for the 3:2 (*left panel*), 3:1 (*middle panel*) and 2:1 (*right panel*) ratios of $\nu_{\rm K}/\nu_r$, for the upper frequencies $\nu_{\rm upp}$ = 168 Hz, 242 Hz, 276 Hz, and 450 Hz (curves from the top in this order) observed in four microquasars (Table 1). Shadows show the range ±5 Hz and arrows indicate the observationally given range of mass for the source (in the case of H 1743-322 [i.e. 242 Hz], the mass is not established yet). Resonances are between radial epicyclic oscillations and some oscillations at Keplerian frequency. The vertical lines in the middle and right panels correspond to $a = 0.479$ and $a = 0.353$, respectively.

frequencies exclude the case $\nu_{\rm K}/\nu_r = 3/2$ for prefered masses of three microquasars (see Table 1 vs. A.4). Another possibility that may come to mind is based on the following idea (Spiegel 2003). When the potential vorticity is conserved, coherent vortices tend to form in pairs with opposite vorticity (Bracco et al. 1998). One can imagine that, in such situation, a resonance between the radial epicyclic frequency and Keplerian orbital frequency is possible because the spatial distance between the two structures that oscillate with the radial frequency depends on the velocity profile of the disk (i.e., on the variations of the Keplerian orbital velocity). In Fig. 8 we plot the prediction of the three possible cases corresponding to $\omega_{\rm upp}/\omega_{\rm down} = 3/2$,

$$\begin{aligned}
&\omega_{\rm upp}{=}3\,\omega_r, \omega_{\rm down} = \omega_{\rm K} = 2\,\omega_r,\\
&\omega_{\rm upp}{=}\omega_{\rm K},\ \omega_{\rm down} = 2\,\omega_r = (2/3)\,\omega_{\rm K},\\
&\omega_{\rm upp}{=}\omega_{\rm K},\ \omega_{\rm down} = \omega_r = (2/3)\,\omega_{\rm K}. \qquad (15)
\end{aligned}$$

4. Conclusions

In the Appendix (A.1−A.12) we present tables summarizing spin-mass combinations implied by the resonance models. Keep in mind that the observed upper frequencies in the microquasars are rather well fit by the relationship (7) found by McClintock & Remillard (2003), $\nu_{\rm upp} = 2.793\,(M_\odot/M_0)$ kHz. Spin implied by this fit is illustrated on the right panel of Fig. 6 for the 3:2 parametric resonance and evaluated in Tables 2 and 3, which include also the discussed forced and "Keplerian" resonances.

The resonance model is rather sensitive to observational constraints; the data already excludes the 3:2 "Keplerian" resonance as a possible explanation of twin peak QPOs in the case of three microquasars. All other resonances discussed in this paper are consistent with the existing data, but it is plausible that future observations may narrow down the choice of a resonance. Future developments in accretion disk theory could also narrow down the choice. For example, it is often argued that the presence of a relativistic jet is a signature of large black hole spin (Blandford & Znajek 1977; see however Ghosh & Abramowicz 1997). Because microquasars do have jets, one would expect that $a \approx 1$ for their black holes. This argument, if proven true, would uniquely point to the 3:2 parametric resonance as the only possible choice for the three microquasars with known masses.

Table 2. Spin implied by fit (7) for given [parametric or forced (3:1, 3:2)] resonance.

Type of resonance		Spin estimate equivalent to the best fit (7)
standard	parametric	0.97
	3:1 forced	0.53
	2:1 forced	0.35
Keplerian	parametric	–
	3:1 forced	0.48
	2:1 forced	0.35

Table 3. Spin implied by fit (7) for given (5:1, 5:2 and 5:3) forced resonance.

Type of resonance		Spin estimate equivalent to the best fit (7)
standard	5:1 forced	0.18
	5:2 forced	0.95
	5:3 forced	–
Keplerian	5:1 forced	0.15
	5:2 forced	0.90
	5:3 forced	–

Different resonances occur at very different resonance radii. Figure 5 shows that accretion disk physics at these radii is also very different. The 3:2 parametric resonance is located at a very outer part of the innermost region of the disk. Discussed forced resonances (giving observed 3:2 ratio) are subsequently closer to the inner edge in the sequence of radii giving $\nu_\theta : \nu_r$ in ratios 5:3, 2:1, 5:2 and the location of the 5:1 resonance is closest to the inner edge of this region. Therefore, the physical excitation mechanism (still unknown) must be very different for different resonances.

If the resonace model is correct, and the kHz double peak QPOs are indeed caused by non-linear resonance in strong gravity, the QPO phenomenon would be of a fundamental importance as a practical test of super-strong gravity. It could also be useful in several astrophysical applications of black hole astrophysics. For example, the $1/M$ scaling of the twin peak QPOs' frequencies with the 3:2 ratio (shown in Fig. 1) was proposed by Abramowicz et al. (2004a) as a method for estimating black hole masses in AGNs and ULXs.

Acknowledgements. We thank J. McClintock, R. Remillard, and R. V. Wagoner for comments. Most of the work reported here was carried out at the UK Astrophysical Fluids Facility (UKAFF) and supported through the European Comission's *Access to Research Infrastructure action of the Improving Human Potential Program*. It is a pleasure to acknowledge the hospitality of the UKAFF staff and of Sir Franciszek Oborski, the Master of Wojnowice Castle, where we have continued our work. Z.S. and G.T. were supported by the Czech GACR grants 202/02/0735 and 205/03/H144, and M.A.A. and W.K. by the Polish KBN grants 2P03D01424 and PBZ-KBN-054/803/2001. Z.S., M.A.A., and G.T. were also supported by the Czech grant MSM 4781305903.

References

Abramowicz, M. A., & Kluźniak, W. 2001, A&A, 374, L19
Abramowicz, M. A., Chen, X. M., Granath, M., & Lasota, J. P. 1976, ApJ, 471, 762
Abramowicz, M. A., Czerny, B., Lasota, J. P., & Szuszkiewicz, E. 1988, ApJ, 332, 646
Abramowicz, M. A., Karas, V., Kluźniak, W., Lee, W., & Rebusco, P. 2003, Publ. Astr Soc. Japan, 55, 467
Abramowicz, M. A., Kluźniak, W., McClintock, J. E., & Remillard, R. A. 2004a, ApJ, 609, L63
Abramowicz, M. A., Kluźniak, W., Stuchlík, Z., & Török, G. 2004b, in Proc. of RAGtime 5: Workshops on black holes and neutron stars, ed. S. Hledík, & Z. Stuchlík, Opava, 14–16/13–15 October 2002/03, Silesian University at Opava
Blandford, R. D., & Znajek, R. L. 1977, MNRAS, 179, 433
Bracco, A., Provenzale, A., Spiegel, E. A., & Yecko, P. 1998, in Theory of Black Hole Accretion Disks, ed. M. A. Abramowicz, G. Björnsson, & J. E. Pringle (Cambridge: Cambridge University Press)
Bursa, M. 2004, in Proc. of RAGtime 5: Workshops on black holes and neutron stars, ed. S. Hledík, & Z. Stuchlík, Opava, 14–16/13–15 October 2002/03, Silesian University at Opava
Bursa, M., Abramowicz, M. A., Karas, V., & Kluźniak, W. 2004, ApJ, 617, 45
Ghosh, P., & Abramowicz, M. A. 1997, MNRAS, 292, 88
Greene, J., Bailyn, Ch. D., & Orosz, J. A. 2001, ApJ, 554, 1290
Greiner, J., Cuby, J. G., & McCaughrean, M. J. 2001, Nature, 414, 522
Homan, J., Miller, J. M., Wijnands, R., et al. 2003, Atel 16 http://integral.rssi.ru/atelmirror/
Horák, J. 2004, in Proc. of RAGtime 5: Workshops on black holes and neutron stars, ed. S. Hledík, & Z. Stuchlík, Opava, 1416/1315 October 2002/03, Silesian University at Opava
Horák, J., Abramowicz, M. A., Karas, V., & Kluźniak, W. 2004, Publ. Astron. Soc. Japan, 56, 819
Kato, S. 2001, Publ. Astron. Soc. Japan, 53, L37
Kato, S. 2001, Publ. Astron. Soc. Japan, 53, L39
Kluźniak, W., & Abramowicz, M. A. 2000, Phys. Rev. Lett., submitted [arXiv:astro-ph/0105057]
Kluźniak, W., & Abramowicz, M. A. 2001, Acta Physica Polonica B 32, 3605 http://th-www.if.uj.edu.pl/acta/vol32/t11.htm
Kluźniak, W., & Abramowicz, M. A. 2002 [arXiv:astro-ph/0203314]
Kluźniak, W., & Abramowicz, M. A. 2004, in X-Ray Timing 2003: Rossi and Beyond, ed. P. Kaaret, F. K. Lamb, & J. Swank (New York: American Institute of Physics), AIP Conf. Proc., 714, 21
Kluźniak, W., Michelson, P., & Wagoner, R. V. 1990, ApJ, 358, 538
Kozłowski, M., Jaroszyński, M., & Abramowicz, M. A. 1978, A&A, 63, 209
Landau, L. D., & Lifshitz, E. M. 1976, Mechanics, 3rd edition (Oxford: Pergamon Press)
Lee, W. H., Abramowicz, M. A., & Kluźniak, W. 2004, ApJ, 603, L93
McClintock, J. E., & Remillard, R. A. 2003 [arXiv:astro-ph/0306213]
McClintock, J. E., & Remillard, R. A. 2004, ApJ, submitted [arXiv:astro-ph/0407025]
Mirabel, I. F., & Rodríguez, L. F. 1998, Nature, 392, 673
Nayfeh, A. H., & Mook, D. T. 1979, Nonlinear Oscillations (New York: Wiley-Interscience)
Nowak, M., & Lehr, D. 1999, in Theory of Black Hole Accretion Disks, ed. M. A. Abramowicz, G. Björnsson, & J. E. Pringle (Cambridge: Cambridge University Press)
Okazaki, A. T., Kato, S., & Fukue, J. 1987, Publ. Astron. Soc. Japan, 39, 457
Orosz, J. A., Groot, P. J., van der Klis, M., et al. 2002, ApJ, 568, 845O
Page, D. N., & Thorne, K. S. 1974, ApJ, 191, 499P
Pringle, J. 1997, MNRAS, 297, 136
Rebusco, P. 2004, Laurea Thesis, University of Trieste
Rebusco, P. 2004, PASJ, 56, 553
Remillard, R. A., Morgan, E. H., McClintock, J. E., Bailyn, C. D., & Orosz, J. A. 1999, ApJ, 522, 397
Remillard, R. A., Muno, M. P., McClintock, J. E., & Orosz, J. A. 2002, ApJ, 580, 1030
Remillard, R. A., Muno, M. P., McClintock, J. E., & Orosz, J. A. 2003, AAS meeting #35, #30.03
Spiegel, E. A. 2003, private communication
Strohmayer, T. E. 2001, ApJ, 552, L49
van der Klis, M. 2000, A&ARv, 38, 717
Török, G., & Stuchlík, Z. 2005, A&A, accepted [arXiv:astro-ph/0502127]

Online Material

Article published by EDP Sciences and available at http://www.edpsciences.org/aa or http://dx.doi.org/10.1051/0004-6361:20047115

Appendix A: Detailed estimate of mass for standard and "Keplerian" parametric and some forced resonance models calculated from observed frequencies ($\nu_{\rm upp}$ – Table 1)

Table A.1. Summary of mass estimates for 3:2 parametric resonance model (Fig. 6).

↓ a		$M/M_\odot$			
		168 Hz in	242 Hz in	276 Hz in	450 Hz in
	r/M	GRS 1915+105	H1743-322	XTE 1550-564	GRO 1655-40
−1.00	15.7	3.25	2.25	1.98	1.21
−0.90	15.3	3.39	2.35	2.06	1.26
−0.80	14.8	3.53	2.45	2.15	1.32
−0.70	143	3.70	2.57	2.25	1.38
−0.60	13.8	3.87	2.69	2.36	1.45
−0.50	13.4	4.07	2.82	2.48	1.52
−0.40	129	4.28	2.97	2.61	1.60
−0.30	12.4	4.52	3.14	2.75	1.69
−0.20	11.8	4.78	3.32	2.91	1.79
−0.10	113	5.08	3.53	3.09	1.90
0.00	10.8	5.42	3.76	3.30	2.02
0.10	10.3	5.80	4.03	3.53	2.16
0.20	9.70	6.24	4.33	3.80	2.33
0.30	9.13	6.75	4.69	4.11	2.52
0.40	8.54	7.36	5.11	4.48	2.75
0.50	7.92	8.10	5.62	4.93	3.02
0.60	7.27	9.02	6.26	5.49	3.37
0.70	6.58	10.2	7.08	6.20	3.81
0.80	5.82	11.8	8.18	7.17	4.40
0.90	4.96	14.1	9.81	8.60	5.28
1.00	3.87	18.3	12.7	11.2	6.85

Table A.2. Summary of mass estimates for 3:1 forced resonance model (Fig. 7 – left).

	$M/M_\odot$			
	168 Hz in	242 Hz in	276 Hz in	450 Hz in
r/M	GRS 1915+105	H1743-322	XTE 1550-564	GRO 1655-40
10.1	6.63	4.60	4.04	2.48
9.79	6.91	4.80	4.21	2.58
9.47	7.21	5.01	4.39	2.69
9.15	7.54	5.23	4.59	2.81
8.82	7.89	5.48	4.80	2.95
8.49	8.28	5.75	5.04	3.09
8.15	8.71	6.05	5.30	3.25
7.81	9.19	6.38	5.59	3.43
7.47	9.71	6.74	5.91	3.63
7.11	10.3	7.15	627	3.85
6.75	11.0	7.61	6.67	4.09
6.38	11.7	8.13	7.13	4.37
6.00	12.6	8.73	7.65	4.69
5.61	13.6	9.42	8.26	5.07
5.20	14.7	10.2	8.97	5.50
4.77	16.1	11.2	9.82	6.02
4.32	17.8	12.4	10.9	6.66
3.83	20.0	13.9	12.2	7.46
3.29	22.7	15.8	13.8	8.49
2.64	26.5	18.4	16.1	9.88
1.39	24.4	16.9	14.8	9.11

In all Tables (A1−A12) the rows are arranged according to increasing spin, always for the same 21 values of a (given in the very first column of Table A1, and repeated for convenience in Tables A3, A5, ...).
Entries in gray correspond to the *observed mass for the given source* within its range of errors (Table 1).
We note that for 3:1 (5:1) forced resonance there is a maximum for the mass prediction at $a \doteq 0.98$ ($a \doteq 0.96$), corresponding to $r/M = 1.86$ ($r/M = 1.93$). Such nonmonotonicity is natural for any forced resonance between the epicyclic frequencies ν_θ, ν_r with $\nu_\theta/\nu_r > 2.18$ (Török & Stuchlík 2005).

Table A.3. Summary of mass estimates for 2:1 forced resonance model (Fig. 7 – right).

↓ a		$M/M_\odot$			
		168 Hz in	242 Hz in	276 Hz in	450 Hz in
	r/M	GRS 1915+105	H1743-322	XTE 1550-564	GRO 1655-40
−1.00	11.9	7.62	5.29	4.64	2.84
−0.90	11.5	7.94	5.51	4.83	2.96
−0.80	11.2	8.29	5.76	5.05	3.10
−0.70	10.8	8.68	6.02	5.28	3.24
−0.60	10.4	9.10	6.31	5.54	3.40
−0.50	10.0	9.56	6.63	5.82	3.57
−0.40	9.63	10.1	6.99	6.12	3.76
−0.30	9.23	10.6	7.37	6.47	3.97
−0.20	8.83	11.2	7.81	6.85	4.20
−0.10	8.42	11.9	8.30	7.27	4.46
0.00	8.00	12.7	8.85	7.76	4.76
0.10	7.57	13.6	9.47	8.31	5.09
0.20	7.13	14.7	10.2	8.94	5.48
0.30	6.67	15.9	11.0	9.68	5.94
0.40	6.20	17.3	12.0	10.6	6.48
0.50	5.71	19.1	13.3	11.6	7.13
0.60	5.19	21.3	14.8	129	7.94
0.70	4.62	24.0	16.7	14.6	8.97
0.80	4.00	27.8	19.3	16.9	10.4
0.90	3.26	33.4	23.2	20.3	12.5
1.00	2.10	43.1	29.9	26.3	16.1

Table A.4. Summary of mass estimates for 3:2 "Keplerian" resonance model (Fig. 8 – left).

	$M/M_\odot$			
	168 Hz in	242 Hz in	276 Hz in	450 Hz in
r/M	GRS 1915+105	H1743-322	XTE 1550-564	GRO 1655-40
14.9	3.40	2.36	2.07	1.27
14.5	3.54	2.46	2.15	1.32
14.1	3.68	2.56	2.24	1.37
13.7	3.84	2.66	2.34	1.43
13.3	4.01	2.78	2.44	1.50
12.9	4.19	2.91	2.55	1.56
12.5	4.39	3.05	2.67	1.64
12.1	4.61	3.20	2.81	1.72
11.7	4.85	3.37	2.95	1.81
11.2	5.12	3.55	3.12	1.91
10.8	5.42	3.76	3.30	2.02
10.4	5.75	3.99	3.50	2.15
9.91	6.13	4.25	3.73	2.29
9.45	6.55	4.55	3.99	2.45
8.97	7.05	4.89	4.29	2.63
8.49	7.62	5.29	4.64	2.84
7.99	8.30	5.76	5.05	3.10
7.47	9.11	6.33	5.55	3.40
6.92	10.1	7.02	6.16	3.78
6.34	11.4	7.91	6.93	4.25
5.72	13.1	9.08	7.96	4.88

Table A.5. Summary of mass estimates for 3:1 "Keplerian" resonance model (Fig. 8 – middle).

↓ a		$M/M_\odot$			
		168 Hz in	242 Hz in	276 Hz in	450 Hz in
	r/M	GRS 1915+105	H1743-322	XTE 1550-564	GRO 1655-40
−1.00	9.94	6.33	4.40	3.85	2.36
−0.90	9.64	6.62	4.60	4.03	2.47
−0.80	9.34	6.93	4.81	4.22	2.59
−0.70	9.03	7.27	5.05	4.43	2.71
−0.60	8.72	7.65	5.31	4.65	2.85
−0.50	8.40	8.06	5.59	4.90	3.01
−0.40	8.08	8.51	5.91	5.18	3.18
−0.30	7.76	9.02	6.26	5.49	3.37
−0.20	7.43	9.59	6.66	5.84	3.58
−0.10	7.09	10.2	7.10	6.23	3.82
0.00	6.75	11.0	7.61	6.67	4.09
0.10	6.40	11.8	8.19	7.18	4.41
0.20	6.04	12.8	8.87	7.78	4.77
0.30	5.67	13.9	9.67	8.48	5.20
0.40	5.29	15.3	10.6	9.32	5.72
0.50	4.89	17.0	11.8	10.4	6.35
0.60	4.47	19.1	13.3	11.7	7.15
0.70	4.02	22.0	15.2	13.4	8.20
0.80	3.53	25.9	18.0	15.7	9.66
0.90	2.97	31.9	22.2	19.4	11.9
1.00	2.25	43.9	30.5	26.7	164

Table A.6. Summary of mass estimates for 2:1 "Keplerian" resonance model (Fig. 8 – right).

	$M/M_\odot$			
	168 Hz in	242 Hz in	276 Hz in	450 Hz in
r/M	GRS 1915+105	H1743-322	XTE 1550-564	GRO 1655-40
11.5	7.59	5.27	4.62	2.84
11.2	7.92	5.50	4.82	2.96
10.8	8.28	5.75	5.04	3.09
10.5	8.66	6.01	5.27	3.23
10.2	9.08	6.31	5.53	3.39
9.81	9.55	6.63	5.81	3.56
9.46	10.1	6.98	6.12	3.75
9.10	10.6	7.37	6.46	3.96
8.74	11.2	7.81	6.85	4.20
8.37	11.9	8.30	7.27	4.46
8.00	12.7	8.85	7.76	4.76
7.62	13.6	9.47	8.31	5.09
7.23	14.7	10.2	8.94	5.48
6.83	15.9	11.0	9.67	5.93
6.42	17.3	12.0	10.5	6.47
5.99	19.0	13.2	11.6	7.10
5.54	21.1	14.7	12.9	7.89
5.07	23.8	16.5	14.5	8.88
4.57	27.3	19.0	16.6	10.2
4.02	32.2	22.4	19.6	12.0
3.38	39.9	27.7	24.3	14.9

Article published by EDP Sciences and available at http://www.edpsciences.org/aa or http://dx.doi.org/10.1051/0004-6361:20047115

Table A.7. Summary of mass estimates for 5:1 forced resonance model.

↓ a		$M/M_\odot$			
		168 Hz in	242 Hz in	276 Hz in	450 Hz in
	r/M	GRS 1915+105	H1743-322	XTE 1550-564	GRO 1655-40
−1.0	9.37	9.02	6.26	5.49	3.37
−0.9	9.08	9.39	6.52	5.72	3.51
−0.8	878	9.80	6.80	5.96	3.66
−0.7	8.48	10.2	7.11	6.23	3.82
−0.6	8.18	10.7	7.43	6.52	4.00
−0.5	7.87	11.2	7.80	6.83	4.19
−0.4	7.56	11.8	8.19	7.18	4.40
−0.3	7.24	12.4	8.63	7.56	4.64
−0.2	6.92	13.1	9.11	7.99	4.90
−0.1	6.59	13.9	9.65	8.46	5.19
0.0	6.25	14.8	10.2	8.99	5.51
0.1	5.91	15.7	10.9	9.58	5.88
0.2	5.55	16.9	11.7	10.3	6.30
0.3	5.19	18.2	12.6	11.0	6.78
0.4	4.81	19.7	13.6	12.0	7.34
0.5	4.41	21.4	14.9	13.0	8.00
0.6	3.99	23.6	16.4	14.3	8.80
0.7	3.54	26.2	18.2	15.9	9.78
0.8	3.03	29.5	20.5	17.9	11.0
0.9	2.42	33.5	23.2	20.4	12.5
1.0	1.13	14.2	9.85	8.64	5.30

Table A.8. Summary of mass estimates for 5:2 forced resonance model.

	$M/M_\odot$			
	168 Hz in	242 Hz in	276 Hz in	450 Hz in
r/M	GRS 1915+105	H1743-322	XTE 1550-564	GRO 1655-40
10.7	3.63	2.52	2.21	1.36
10.3	3.79	2.63	2.31	1.41
10.0	3.96	2.75	2.41	1.48
9.67	4.14	2.87	2.52	1.54
9.32	4.33	3.01	2.64	1.62
8.97	4.55	3.16	2.77	1.70
8.62	4.79	3.32	2.91	1.79
8.26	5.05	3.51	3.07	1.89
7.90	5.34	3.71	3.25	2.00
7.52	5.67	3.94	3.45	2.12
7.14	6.04	4.19	3.68	2.26
6.75	6.46	4.49	3.93	2.41
6.35	6.94	4.82	4.23	2.59
5.94	7.51	5.21	4.57	2.80
5.51	8.17	5.67	4.97	3.05
5.06	8.96	622	5.46	3.35
4.59	9.94	6.90	6.05	3.71
4.07	11.2	7.76	6.80	4.17
3.50	12.8	8.90	7.80	4.78
2.82	15.1	10.5	9.20	5.64
1.61	16.9	11.7	10.3	6.31

Table A.9. Summary of mass estimates for 5:3 forced resonance model.

↓ a		$M/M_\odot$			
		168 Hz in	242 Hz in	276 Hz in	450 Hz in
	r/M	GRS 1915+105	H1743-322	XTE 1550-564	GRO 1655-40
−1.0	13.8	2.40	1.66	1.46	0.895
−0.9	13.4	2.50	1.74	1.52	0.934
−0.8	13.0	2.61	1.81	1.59	0.975
−0.7	12.5	2.73	1.90	1.66	1.02
−0.6	12.1	2.86	1.99	1.74	1.07
−0.5	11.7	3.01	2.09	1.83	1.12
−04	11.2	3.17	2.20	1.93	1.18
−0.3	10.8	3.35	2.32	2.04	1.25
−0.2	10.3	3.54	2.46	2.16	1.32
−0.1	9.85	3.77	2.61	2.29	1.41
0.0	9.38	4.02	2.79	2.45	1.50
0.1	8.89	4.30	2.99	2.62	1.61
0.2	8.39	4.64	3.22	2.82	1.73
0.3	7.87	5.02	3.49	3.06	1.88
0.4	7.34	5.48	3.81	3.34	2.05
0.5	6.78	6.04	4.19	3.68	2.26
0.6	6.19	6.73	4.68	4.10	2.51
0.7	5.56	7.63	5.30	4.65	2.85
0.8	4.86	8.85	6.15	5.39	3.31
0.9	4.06	10.7	7.42	6.51	3.99
1.0	2.94	14.2	9.85	8.64	5.30

Table A.10. Summary of mass estimates for 5:1 "Keplerian" resonance model.

	$M/M_\odot$			
	168 Hz in	242 Hz in	276 Hz in	450 Hz in
r/M	GRS 1915+105	H1743-322	XTE 1550-564	GRO 1655-40
9.32	8.41	5.84	5.12	3.14
9.03	8.80	6.11	5.35	3.28
8.73	9.22	6.40	5.61	3.44
8.44	9.68	6.72	5.90	3.62
8.14	10.2	7.08	6.21	3.81
7.84	10.8	7.47	6.55	4.02
7.53	11.4	7.90	6.93	4.25
7.22	12.1	8.38	7.35	4.51
6.90	12.9	8.93	7.83	4.80
6.58	13.7	9.54	8.37	5.13
6.25	14.8	10.2	8.99	5.51
5.91	15.9	11.1	9.70	5.95
5.57	17.3	12.0	10.5	6.46
5.21	18.9	131	11.5	7.07
4.84	20.9	14.5	12.7	7.80
4.45	23.3	16.2	14.2	8.71
4.04	26.4	18.4	16.1	9.87
3.60	30.6	21.3	18.6	11.4
3.11	36.6	25.4	22.3	13.7
2.54	46.6	32.3	28.4	17.4
1.68	72.4	50.3	44.1	27.0

Table A.11. Summary of mass estimates for 5:2 "Keplerian" resonance model.

↓ **a**		$M/M_\odot$			
		168 Hz in	242 Hz in	276 Hz in	450 Hz in
	r/M	GRS 1915+105	H1743-322	XTE 1550-564	GRO 1655-40
−1.0	10.4	3.53	2.45	2.15	1.32
−0.9	10.1	3.68	2.56	2.24	1.38
−0.8	9.81	3.85	2.68	2.35	1.44
−0.7	9.49	4.04	2.81	2.46	1.51
−0.6	9.17	4.24	2.95	2.58	1.58
−0.5	8.84	4.47	3.10	2.72	1.67
−0.4	8.52	4.72	3.27	2.87	1.76
−0.3	8.18	4.99	3.47	3.04	1.86
−0.2	7.84	5.30	3.68	3.23	1.98
−0.1	7.50	5.65	3.92	3.44	2.11
0.0	7.14	6.04	4.19	3.68	2.26
0.1	6.78	6.49	4.51	3.95	2.42
0.2	6.41	7.02	4.87	4.27	2.62
0.3	6.03	7.63	5.30	4.64	2.85
0.4	5.64	8.36	5.80	5.09	3.12
0.5	5.23	9.25	6.42	5.63	3.45
0.6	4.80	10.4	7.20	6.31	3.87
0.7	4.35	11.8	8.20	7.19	4.41
0.8	3.86	13.8	9.57	8.39	5.14
09	3.30	16.7	11.6	10.2	6.24
1.0	2.63	22.0	15.2	13.4	8.20

Table A.12. Summary of mass estimates for 5:3 "Keplerian" resonance model.

	$M/M_\odot$			
	168 Hz in	242 Hz in	276 Hz in	450 Hz in
r/M	GRS 1915+105	H1743-322	XTE 1550-564	GRO 1655-40
13.2	2.46	1.71	1.50	0.920
12.8	2.56	1.78	1.56	0.957
12.5	2.67	1.86	1.63	0.998
12.1	2.79	1.94	1.70	1.04
11.7	2.92	2.03	1.78	1.09
11.3	3.06	2.13	1.86	1.14
11.0	3.22	2.23	1.96	1.20
10.6	3.39	2.35	2.06	1.26
10.2	3.57	2.48	2.18	1.33
9.78	3.78	2.63	2.30	1.41
9.38	4.02	2.79	2.45	1.50
8.96	4.28	2.97	2.61	1.60
8.54	4.58	3.18	2.79	1.71
8.11	4.93	3.42	3.00	1.84
7.67	5.33	3.70	3.25	1.99
7.21	5.81	4.03	3.53	2.17
6.74	6.38	4.43	3.88	2.38
6.24	7.08	4.92	4.31	2.64
5.72	7.97	5.53	4.85	298
5.16	9.14	6.35	5.57	3.41
4.54	10.8	7.50	6.57	4.03

Article published by EDP Sciences and available at http://www.edpsciences.org/aa or http://dx.doi.org/10.1051/0004-6361:20047115